Labeling for UWB Ranging in Weak NLOS Conditions

Philipp Peterseil, David Märzinger, Bernhard Etzlinger, Andreas Springer

Johannes Kepler University, Linz, Austria, {firstname.lastname}@jku.at

***Abstract*—A stepwise feature labeling method for UWB ranging is presented, which allows better separation of LOS and NLOS components in the training data. The packet-by-packet range error evaluation is used as input of the labeling function instead of the conventionally used double-sided two-way ranging result which relies on a cycle of three packets. To assess the packet-wise error, a two-step synchronization scheme is proposed. First, the clock model between anchor and tag is estimated by a least-squares approach. Second, the remaining bias is corrected by determining the time-shift between the channel impulse responses recorded by both nodes. The evaluation of measurement data shows a significant improvement in classification between LOS and NLOS, as well as slightly improved ranging accuracy when used to train a binary classifier.**

***Index Terms*—UWB ranging, LOS/NLOS detection, double-sided two-way ranging, labeling.**

I. Introduction

Time of flight (ToF) is a key measurement for precise localization. In ultra-wideband (UWB) radios, the most prominent principle to obtain the ToF is the double-sided two-way ranging (DS-TWR) [1]. The scheme requires the exchange of a cycle of three ranging packets and the calculation using the corresponding recorded transmit and estimated receive times. The obtained cycle-wise ToF estimate is thus a weighted average of the three individual packet ToFs.

The main source of error in indoor localization is imposed by multipath and non-line-of-sight (NLOS) propagation. A body of work can be found that recently addressed this problem in model free approaches [2]–[6]. In common, they require labeled training data to determine machine learning parameters in an offline phase to then perform an NLOS detection or error mitigation strategy in the online phase. The data comprises the estimated ToF and channel related features [4], [7]. The labels of the training data are obtained through the ranging error which is proportional to the difference between the estimated and the expected ToF. However, in weak NLOS environments labeling errors are introduced due to application of DS-TWR.

Weak NLOS [8]–[10] manifests in UWB ranging by sometimes measuring ToF of the direct path (i.e., the true distance) and sometimes the ToF of a reflection path. This usually happens at signal levels of the direct path that are close to the detection threshold of the leading edge (LDE) algorithm,

This work was supported in part by the Linz Center of Mechatronics (LCM) in the framework of the Austrian COMET-K2 programme. The first and the second author have contributed equally to this work.

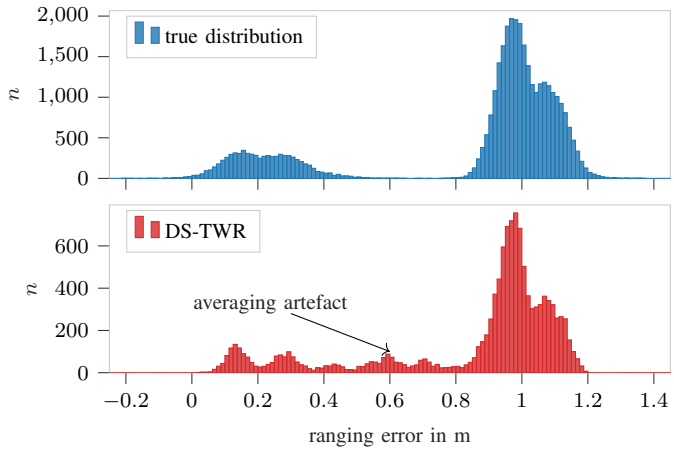

Fig. 1: Histogram of ranging error in weak NLOS (see *test set 1* in Sec. IV). Ranging error (Top:) when individual packets are considered, (Bottom:) for cycle-wise DS-TWR ranging.

which is implemented as blackbox algorithm in commercially available UWB receivers (cf. [11]). If all packets are detected on the direct path or on the reflection path, either the distance of the direct path or the distance of the reflected path is obtained. However, if only one or two packets within the DS-TWR cycle are misdetected, an averaging effect of direct and reflection path occurs (see Fig. 1). Such averaging artefacts occur mainly in weak NLOS and make it difficult to correctly label LOS measurements when assessing the ranging error.

In this work we propose a labeling scheme for weak NLOS scenarios. It mitigates the averaging in the training data by evaluating the ToF of each DS-TWR packet with a two-step clock synchronization method. The so-obtained labels yield a better separation of LOS and NLOS classes.

II. Range-based Labeling

Knowing that the propagation path is obstructed, data points can either be labeled by external knowledge, i.e. ray tracing [5], [6], or labeled based on ranging error [6]. In indoor localization, only the latter is feasible due to the appearance of weak NLOS in complex environments, where distance distributions as in Fig. 1 are observed. Such distributions occur for example if objects like wooden boards, shelfs, office equipment, humans, etc. attenuate the direct path.

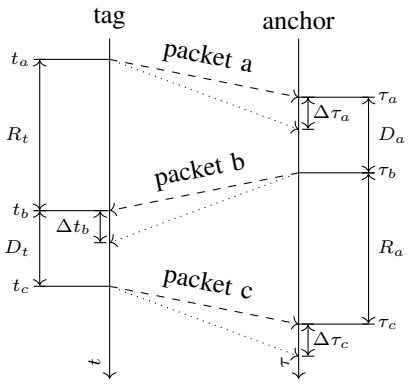

Fig. 2: DS-TWR message exchange scheme.

A. DS-TWR scheme

The DS-TWR is the most widely used ranging scheme and was introduced to minimize the effect of clock synchronization errors in the ranging [1]. In the scheme, a cycle of three packets a, b, c is exchanged between asynchronous tag and anchor devices, as depicted in Fig. 2. Tag and anchor, respectively, record the time stamps t_i and τ_i, $i \in \{\mathrm{a}, \mathrm{b}, \mathrm{c}\}$. While the transmit time stamps t_a, τ_b, t_c are recorded precisely, the receive time stamps τ_a, t_b, τ_c are estimated from the LDE algorithm. The time of flight is estimated [1] by

$$\begin{aligned}\hat{t}_{\mathrm{TOF}} &= \frac{(\tau_c - \tau_b)(t_b - t_a) - (\tau_b - \tau_a)(t_c - t_b)}{-t_a - \tau_a + t_c + \tau_c} \\ &= \frac{R_a\, R_t - D_a\, D_t}{R_a + R_t + D_a + D_t}\,, \end{aligned} \tag{1}$$

using the interval definitions as in Fig. 2. The distance estimate is then obtained by $\hat{d} = c\,\hat{t}_{TOF}$, with c being the speed of light.

The misdetection of individual receive time stamps by $\Delta\tau_\mathrm{a}$, Δt_b, $\Delta\tau_\mathrm{c}$ (e.g., caused by weak NLOS), contributes to the overall ToF estimation error by

$$\Delta\hat{t}_{\mathrm{TOF}} \approx \frac{\partial\hat{t}_{\mathrm{TOF}}}{\partial\tau_\mathrm{a}}\Delta\tau_\mathrm{a} + \frac{\partial\hat{t}_{\mathrm{TOF}}}{\partial t_\mathrm{b}}\Delta t_\mathrm{b} + \frac{\partial\hat{t}_{\mathrm{TOF}}}{\partial\tau_\mathrm{c}}\Delta\tau_\mathrm{c}\,.$$

In case of symmetric conditions $R_t = R_a = R$, $D_t = D_a = D$ it can be found that the weights $\partial\hat{t}_{\mathrm{TOF}}/\partial\tau_\mathrm{a} = \partial\hat{t}_{\mathrm{TOF}}/\partial\tau_\mathrm{c} = 0.25$ and $\partial\hat{t}_{\mathrm{TOF}}/\partial t_\mathrm{b} = 0.5$, which indicates that a detection error of packet b has twice the impact on the the overall error compared to packets a and c. In the asymmetric implementation as used in this paper (see Sec. IV), the weights are $\partial t_{\mathrm{TOF}}/\partial\tau_\mathrm{a} = \partial t_{\mathrm{TOF}}/\partial\tau_\mathrm{c} = 0.2$ and $\partial t_{\mathrm{TOF}}/\partial t_\mathrm{b} = 0.6$.

B. Features for NLOS Detection

Using the Qorvo DW1000 UWB transceiver, multiple quantities[1] can be recorded besides the receive time-stamp. An example of measurement values for a single packet reception is depicted in Fig. 3.

From these measurements, a number of commonly known features are used. These are: the three power features - received signal power level P_{RX}, first path power level P_{FP} [11] and accumulator saturation M_c [12]; calculated from the CIR, four physical features - maximum amplitude h_{max}, mean excess delay τ_{MED}, delay spread σ_{DS} and Kurtosis κ [7, Eqs. (2)-(7)]; two probabilistic features - probability of NLOS p_{NLOS} and probability of undetected early path p_{UEP} [12]. Together with the receive timestamp `RX_STAMP`, ten features are available.

[1]The register values `ACC_MEM`, `STD_NOISE`,`FP_INDEX`,`FP_AMPL1..3`, `RX_STAMP`, `LDE_THRESH`, `LDE_PPINDEX`, `PP_AMPL`, `NTM`, `RXPACC` are explained in detail in [11].

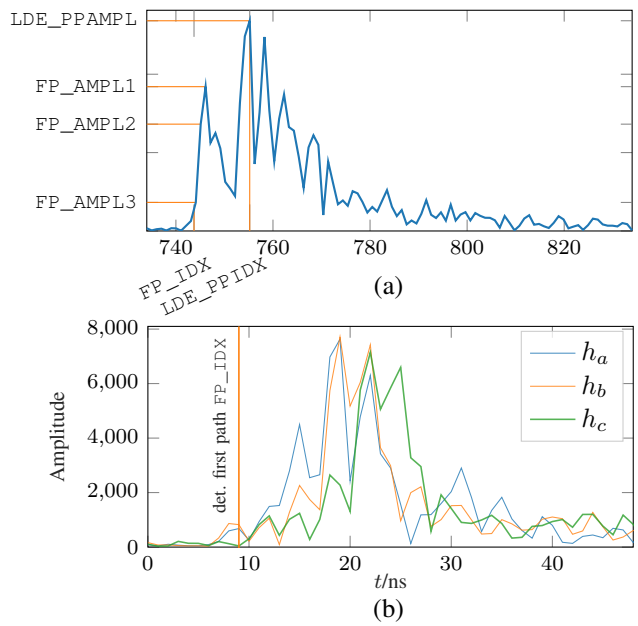

Fig. 3: (a) Absolute CIR values from `ACC_MEM` and related DW1000 parameters. The time axis corresponds to the memory index. (b) CIR overlay of 3 DS-TWR packets, aligned to detected first path. The first path detection was incorrect at packets {a,b} and correct at c, yielding to averaging artefacts.

C. Cycle-wise and Step-wise Labeling

Consider a training data set of N DS-TWR cycles, denoted by $i \in \{0, N-1\}$, with the collected feature vectors $\mathbf{x}_{j,i} \in \mathbb{R}^{10}$, $j \in \{\mathrm{a}, \mathrm{b}, \mathrm{c}\}$. In a conventional approach, a label y is computed cyclewise, i.e.,

$$y_i = \Lambda\big(c\,\hat{t}_{\mathrm{TOF},i} - d_{\mathrm{true}}\big)\,, \tag{2}$$

where $\Lambda(\cdot)$ is a labeling function, $c\,\hat{t}_{\mathrm{TOF},i}$ the cycle-wise distance estimate according to (1), and d_{true} the ground truth distance. The so-obtained label y_i can be used cyclewise, i.e., $(\mathbf{x}_i, y_i)$ with $\mathbf{x}_i = \big[\mathbf{x}_{\mathrm{a},i}^{\mathrm{T}}, \mathbf{x}_{\mathrm{b},i}^{\mathrm{T}}, \mathbf{x}_{\mathrm{c},i}^{\mathrm{T}}\big]^{\mathrm{T}}$ being the stacked version of the individual feature vectors, as depicted in Fig. 4(a). Alternatively–to reduce training complexity–the obtained y_i can be used to label each step, i.e., $(\mathbf{x}_{j,i}, y_i)$ as depicted in Fig. 4(b). While each packet of the DS-TWR is identically labeled, the feature dimension is kept low. The biggest drawback of the conventional labeling is the error from the averaging artefacts. Therefore, in this work we introduce a method that enables the estimation of the packet-ToFs $\hat{t}_{\mathrm{TOF},j,i}$ to then label each packet by

$$\hat{y}_{j,i} = \Lambda\big(c\,\hat{t}_{\mathrm{TOF},j,i} - d_{\mathrm{true}}\big)\,. \tag{3}$$

After labeling, the tuples $(\mathbf{x}_{j,i}, \hat{y}_{j,i})$ are available for further processing. The concept of packet-wise labeling is sketched in Fig. 4(c).

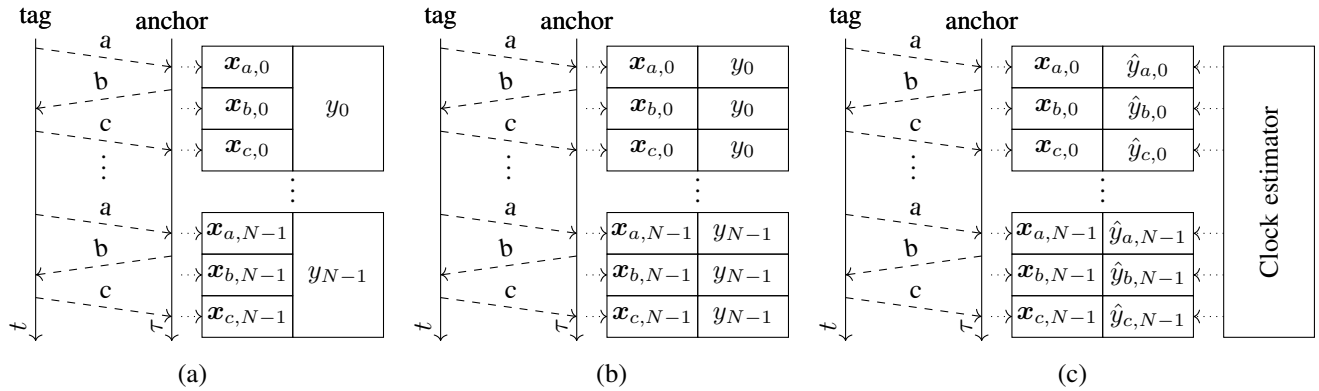

Fig. 4: Labeling options for DS-TWR: (a) conventional cyclic labeling - using a single label for the stacked features; (b) conventional stepwise labeling - labeling the features of each received packet with a copy of the cyclic label; (c) proposed stepwise labeling - computing a different label for each received packet.

Here, the labeling function Λ is chosen as a step function with threshold ζ and ranging error e as

$$\Lambda(e) = \begin{cases} 1 & \text{if } e < \zeta \\ 0 & \text{otherwise}\,. \end{cases} \tag{4}$$

III. Advanced Step-wise Labeling

The proposed packetwise ToF estimation for labeling the training data applies a clock parameter estimation and a timing refinement based on the captured CIR.

A. Clock Parameter Estimation

Consider anchor time τ as reference time that maps to the tag time $t = \chi(\tau)$ using the clock model

$$\chi(\tau) = \frac{a}{2}\tau^2 + v\,\tau + t_0\,.$$

The ToFs for the packets of a cycle i can be expressed by $t_{\text{TOF}} = \chi(\tau_{\text{a},i}) - t_{\text{a},i} + w_{\text{a},i}$, $t_{\text{TOF}} = t_{\text{b},i} - \chi(\tau_{\text{b},i}) + w_{\text{b},i}$ and $t_{\text{TOF}} = \chi(\tau_{\text{c},i}) - t_{\text{c},i} + w_{\text{c},i}$, where w denotes noise. Rewritten in matrix form yields

$$\underbrace{\begin{bmatrix} t_{a,0} \\ \vdots \\ t_{a,N-1} \\ t_{b,0} \\ \vdots \\ t_{b,N-1} \\ t_{c,0} \\ \vdots \\ t_{c,N-1} \end{bmatrix}}_{\triangleq \mathbf{t}} = \underbrace{\begin{bmatrix} {\tau_{a,0}}^2 & \tau_{a,0} & 1 & -1 \\ \vdots & \vdots & \vdots & \vdots \\ {\tau_{a,N-1}}^2 & \tau_{a,N-1} & \vdots & -1 \\ {\tau_{b,0}}^2 & \tau_{b,0} & \vdots & 1 \\ \vdots & \vdots & \vdots & \vdots \\ {\tau_{b,N-1}}^2 & \tau_{b,N-1} & \vdots & 1 \\ {\tau_{c,0}}^2 & \tau_{c,0} & \vdots & -1 \\ \vdots & \vdots & \vdots & \vdots \\ {\tau_{c,N-1}}^2 & \tau_{c,N-1} & 1 & -1 \end{bmatrix}}_{\triangleq \mathbf{H}} \underbrace{\begin{bmatrix} a/2 \\ v \\ t_0 \\ t_{\text{TOF}} \end{bmatrix}}_{\triangleq \boldsymbol{\theta}} + \mathbf{w}\,.$$

The least-squares solution for the unknown parameters $\boldsymbol{\theta}$ is

$$\hat{\boldsymbol{\theta}} = (\mathbf{H}^{\mathrm{T}}\mathbf{H})^{-1}\mathbf{H}^{\mathrm{T}}\mathbf{t}\,, \tag{5}$$

which is the optimal solution for white Gaussian noise $\mathbf{w}$.

B. Estimation Bias

Since the measurement noise $\mathbf{w}$ is not zero-mean in obstructed environments (cf. Fig. 1), the resulting bias in (5) has to be analyzed. Substituting the relation $\mathbf{t} = \mathbf{H}\,\boldsymbol{\theta} + \mathbf{w}$ into (5) and taking the expectation yields

$$\begin{aligned} \mathbb{E}\{\hat{\boldsymbol{\theta}}\} &= \mathbb{E}\{(\mathbf{H}^{\mathrm{T}}\mathbf{H})^{-1}\mathbf{H}^{\mathrm{T}}\mathbf{t}\} \\ &= \mathbb{E}\{(\mathbf{H}^{\mathrm{T}}\mathbf{H})^{-1}\mathbf{H}^{\mathrm{T}}(\mathbf{H}\,\boldsymbol{\theta} + \mathbf{w})\} \\ &= \boldsymbol{\theta} + \underbrace{(\mathbf{H}^{\mathrm{T}}\mathbf{H})^{-1}\mathbf{H}^{\mathrm{T}}\mathbb{E}\{\mathbf{w}\}}_{\text{bias } b}\,. \end{aligned}$$

Denoting the bias on the individual packets by $\mathbb{E}\{w_{j,i}\} = \mu_j$, $j \in \{\text{a}, \text{b}, \text{c}\}$, the relation

$$\boldsymbol{b} = \begin{bmatrix} 0 \\ \frac{N\,\eta\,(\mu_{\text{c}} - \mu_{\text{a}})}{3s_2 + 2N\,\eta^2} \\ \frac{\mu_{\text{a}} + \mu_{\text{c}}}{4} - \frac{\mu_{\text{b}}}{2} \\ -\frac{\mu_{\text{a}} + \mu_{\text{c}}}{4} - \frac{\mu_{\text{b}}}{2} \end{bmatrix} \approx \begin{bmatrix} 0 \\ 0 \\ \frac{\mu_{\text{a}} + \mu_{\text{c}}}{4} - \frac{\mu_{\text{b}}}{2} \\ -\frac{\mu_{\text{a}} + \mu_{\text{c}}}{4} - \frac{\mu_{\text{b}}}{2} \end{bmatrix}, \tag{6}$$

can be found for symmetric message exchange with interval $\eta = \tau_{\text{b},i} - \tau_{\text{a},i} = \tau_{\text{c},i} - \tau_{\text{b},i}$ and with $s_2 \triangleq \sum_{i=0}^{N-1} \left(\tau_{\text{b},i} - \mathbb{E}\{\tau_{\text{b},i}\}\right)^2$. The approximation in (6) assumes realistic clock parameters (in the magnitude of ppm) and practical time intervals (in the magnitude of seconds). It can be concluded that bias due to NLOS mainly effects t_0, referred to as b_t, and t_{TOF}.

C. Clock Refinement

To eliminate the clock offset bias and to improve the accuracy of the ToF estimation for each packet, the following refinement based on the recorded CIR is proposed:

1) Estimate clock model (5) and map anchor time to tag time. *Note: A clock bias b_t remains at this stage.*
2) Shift all CIRs with the estimated TX time as origin. *Note: The remaining b_t will appear in opposing directions on anchor and tag.*
3) Average CIR from anchor to tag and from tag to anchor.
4) Calculate average shift between averages CIRs.
5) Refine the clock offset estimate.

These steps are visualized in Fig. 5 and detailed below. For CIR processing, the `ACC_MEM` time resolution of 1 ns is increased by upsampling factor $u = 64$ to match the

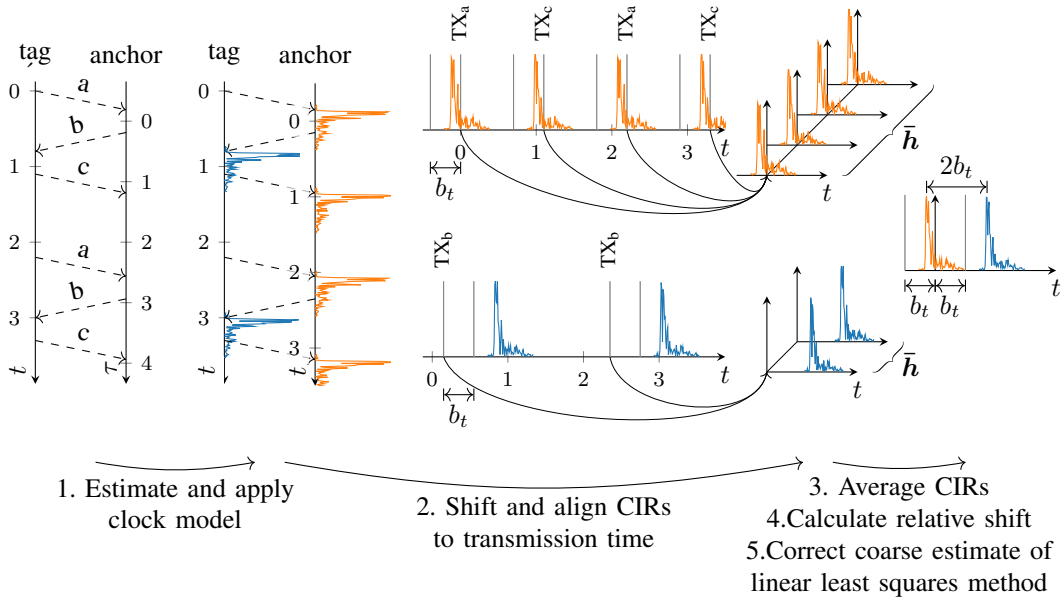

Fig. 5: Clock Estimation Process

RX_STAMP resolution of $T_s = 15.8\,\text{ps}$. In time basis t, the upsampled CIR recorded at the receiver $h^{(\text{RX})}$ is shifted to estimated transmission time $h^{(\text{TX})}$ by

$$h^{(\text{TX})}[k] = h^{(\text{RX})}[k - \Delta n + \texttt{FP\_INDEX} \cdot u]\,,$$

where $\Delta n \triangleq \lfloor \hat{t}_{\text{TOF}}/T_s \rceil$ and index k w.r.t. estimated transmission time. Third, all CIRs from anchor to tag, i.e., $h^{(\text{TX})}_{\text{a},j}[k]$ and $h^{(\text{TX})}_{\text{c},j}[k]$, and tag to anchor $h^{(\text{TX})}_{\text{b},j}[k]$ are averaged

$$\bar{h}^{(\text{TX})}_{\text{T}\to\text{A}}[k] = \frac{1}{2N}\sum_{j=0}^{N-1} h^{(\text{TX})}_{\text{a},j}[k] + h^{(\text{TX})}_{\text{c},j}[k]\,,$$

$$\bar{h}^{(\text{TX})}_{\text{A}\to\text{T}}[k] = \frac{1}{N}\sum_{j=0}^{N-1} h^{(\text{TX})}_{\text{b},j}[k]\,.$$

The relative time shift Δk (corresponding to $2b_t$) between $\bar{h}^{(\text{TX})}_{\text{T}\to\text{A}}[k]$ and $\bar{h}^{(\text{TX})}_{\text{A}\to\text{T}}[k]$ is found by

$$\Delta k = \arg\max_j \left\langle \bar{h}^{(\text{TX})}_{\text{T}\to\text{A}}[k], \bar{h}^{(\text{TX})}_{\text{A}\to\text{T}}[k-j] \right\rangle .$$

Finally, the refined clock offset estimate $\hat{t}_0^*$ is obtained by

$$\hat{t}_0^* = \hat{t}_0 - \frac{\Delta k}{2}\,.$$

D. Packet-wise ToF Estimation

With the estimated clock model

$$\hat{\chi}(\tau) = \frac{\hat{a}}{2}\tau^2 + \hat{v}\,\tau + \hat{t}_0^*\,,$$

it is now possible to determine the ToF for each packet with

$$\hat{t}_{\text{TOF,a},i} = \hat{\chi}(\tau_{\text{a},i}) - t_{\text{a},i}\,, \tag{7}$$

$$\hat{t}_{\text{TOF,b},i} = t_{\text{b},i} - \hat{\chi}(\tau_{\text{b},i})\,, \tag{8}$$

$$\hat{t}_{\text{TOF,c},i} = \hat{\chi}(\tau_{\text{c},i}) - t_{\text{c},i}\,, \tag{9}$$

and consequently the distance and ranging error. Fig. 6(a) depicts a comparison of the stepwise and the cyclic ranging error

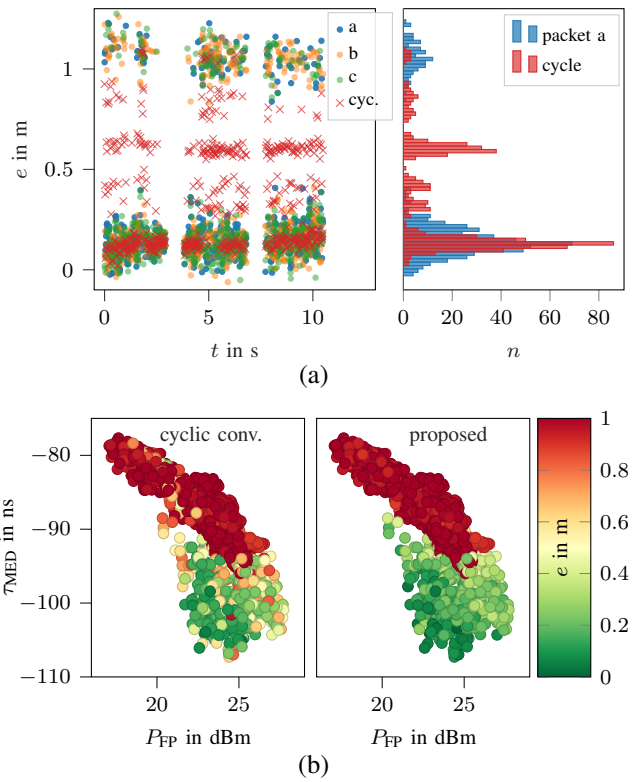

Fig. 6: Ranging error e from cyclic vs. proposed ToF/range estimation: (a) sequence over time and in histogram; (b) in 2-D feature space.

e. It can be observed that the averaging artefacts disappear for the proposed step-wise procedure. In the feature space, as examplary depicted for $\mathbf{x} = \left[P_{\text{FP}}, \tau_{\text{MED}}\right]^{\text{T}}$ in Fig. 6(b), a better separation w.r.t. the ranging error can be observed as well. The ToF estimates (7)–(9) can be now used for labeling the training data through (3).

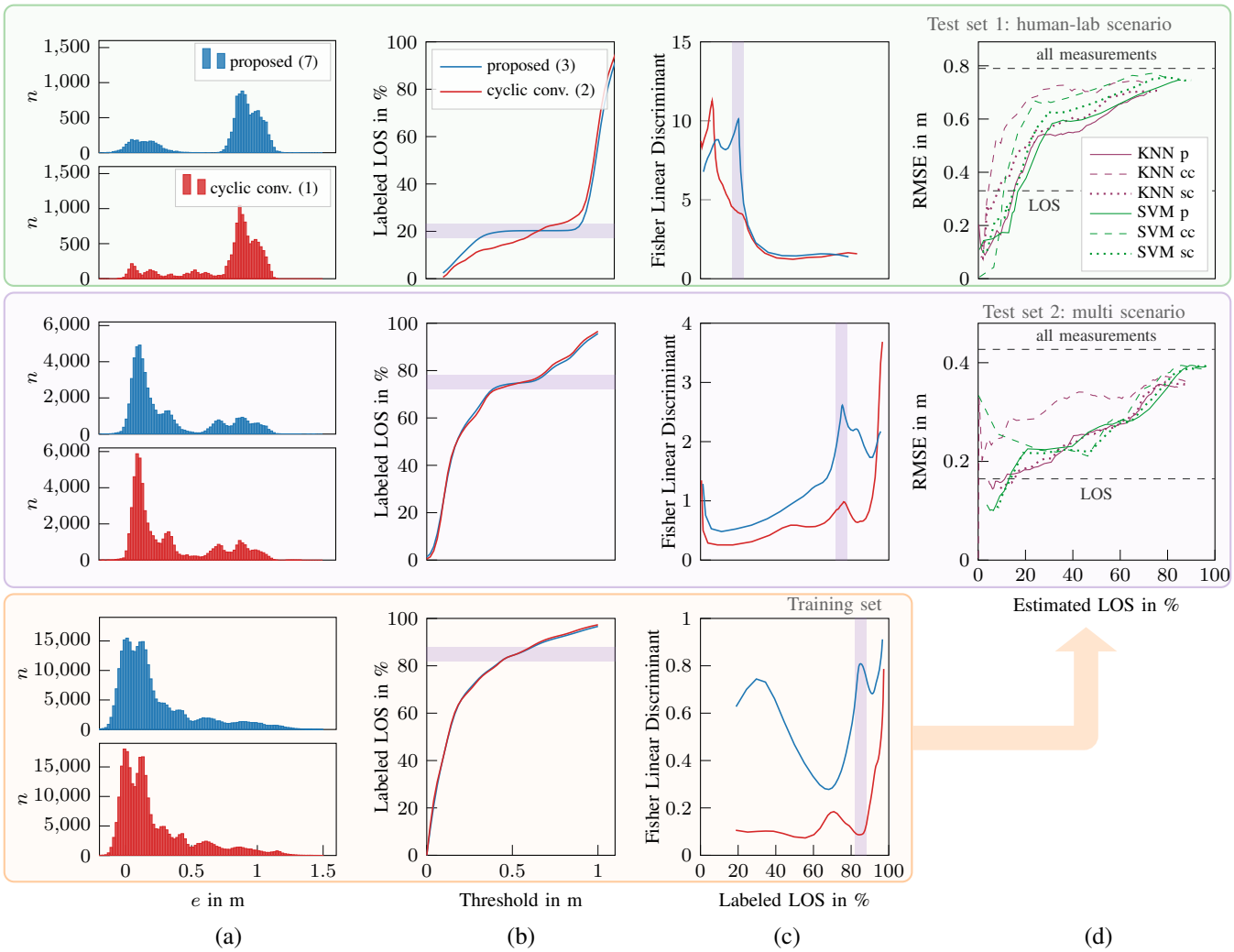

Fig. 7: Evaluation on three data sets (top: test set 1, middle: test set 2, bottom: training set) of the proposed labeling scheme: (a) histograms of proposed packet-wise computation of ranging error vs. conventional cyclic DS-TWR computation; (b) influence of the labeling function threshold ζ on the proportion of LOS samples; (c) separation of LOS and NLOS classes; (d) RMSE of DS-TWR results after binary classifier that was trained with labeled training set.

IV. Evaluation

The proposed stepwise labeling approach is tested on measurement data and compared to the conventional cyclic and the conventional stepwise approach.

A. Evaluation Data

In total, 400k DS-TWR cycles were collected and structured in 36 data sets (available at [13]). The data sets differ in weak NLOS environment (15 in corridor, 12 in lab, 5 outdoors, 4 in anechoic chamber), in ground truth distance (1, 3, 5 and 8 m), and in obstacle on the LOS path (none, non-conductive wooden wall, conductive flipchart, human). Per data set, 20 relative angular orientations differing by 18° were adjusted and for each 200 DS-TWR cycles between 3 node pairs were performed. For each DS-TWR packet, 10 features (see Sec. II-B) and the CIR were measured.

The evaluation data is partitioned into two disjoint data set groups for training and testing consisting of n_{train} and n_{test} data sets, as indicated by the $n_{\text{train}}/n_{\text{test}}$ tuples in Tab. I. All 24 data sets from the training group are referred to as the *training set*. From the testing group, the single scenario "lab-human" is used in *test set 1*, which shows significantly good results. Note that the obstacle/environment combination of lab/human does not exist in the training data. All data sets of the testing group are referred to as *test set 2*, in which a combination of obstacles, environments and distances is included.

TABLE I: Composition of training and testing data sets.

#datasets $n_{\text{train}}/n_{\text{test}}$	anechoic chamber	corridor	lab	outdoor	Σ
LOS	2/0	2/1	2/1	2/0	8/2
human	0/0	3/0	0/1	2/0	5/1
wood	0/0	3/0	2/0	0/0	5/0
flipchart	0/0	2/1	2/0	0/0	4/1
monitor	0/0	0/0	2/1	0/0	2/1
Σ	2/0	10/2	8/3	4/0	24/5

B. Ranging Error

In the histograms in Fig. 7(a), the proposed ToF computation (7) is compared to the conventional cyclic DS-TWR (1) via the distance error e. For the two test data sets (first two rows), the proposed scheme is able to separate the error

distribution into two distinct groups. These groups can be interpreted as LOS and NLOS. For the training set (third row), the histogram does not show a visible improvement in separation. This is explained by multiple overlapping NLOS groups that appear in the 24 individual data sets.

C. Label Quality

We further investigate the proposed scheme when used for LOS/NLOS labeling according to (4). Fig. 7(b) depicts the relation between threshold parameter ζ of (4) and the relative amount of LOS labeled data points. The highlighted plateaus in both test sets (top 2 rows) for the proposed stepwise scheme confirm the separation seen in the histograms, i.e., although the threshold is increased, no new samples are added to the LOS set. In the training set (row 3), as already suggested by the histogram of ranging error, neither a clear separation nor an improvement of the proposed scheme is visible. For further investigation on class separation in labeling, the Fisher Linear Discriminant [14] is compared in Fig. 7(c). In all three data sets, a better separation–indicated by higher values of the discriminant–can be observed for a reasonable percentage of labeled LOS values. Note that the high discriminant value of the conventional scheme in test set 1 (red line in top row) is at about 6% labeled LOS, i.e., a possibly high number of LOS measurements is neglected. Overall, Fig. 7(b) and (c) indicate that the proposed scheme improves class separation on all data sets when used for labeling.

D. Detection Performance

Finally, we evaluate how the proposed labeling approach improves the performance of LOS/NLOS detection schemes. Since no ground-truth data on LOS/NLOS paths is available, the detection performance is evaluated through the root mean square error (RMSE) of DS-TWR results from estimated LOS packets. Thereby, two detection algorithms, k-nearest neighbors (KNN) and support vector machine (SVM), respectively, are trained either with the proposed stepwise (p), the conventional cyclic (cc) or the conventional stepwise (sc) labeled training data set and tested on test set 1 and 2. Fig. 7(d) depicts RMSE versus percentage of estimated LOS packets, and compares to the RMSE of all measurements (corresponds to worst case) and, respectively, to the RMSE of LOS measurements if labeled with the best separation threshold (corresponds to best case). Remarkably, on test set 1 (top row) the detectors with the proposed labeled training data show an improved RMSE performance for both detector types over almost the entire range of % estimated LOS, i.e., the detected LOS samples have lower ranging errors. Cyclic conventional is the worst choice for labeling (up to 20 cm worse), followed by stepwise conventional (up to 10 cm worse). On test set 2 (second row), a clear advantage of the proposed labeling scheme can not be confirmed. For KNN, learning with the proposed labeling scheme clearly outperforms (by up to 15cm) the conventional cyclic method. However, it is as good as the conventional stepwise labeling. For SVM, all three labeling methods perform almost equally for a wide range of % estimated LOS. The results on these two test sets suggest that the stepwise labeling is always preferable for KNN, which is explained by a reduced feature dimension. For SVM, a similar observation holds, while the difference is not so clear. The proposed stepwise labeling method either performs better or almost equal for detection. Further investigations, not depicted here, confirm these results.

V. Conclusion

We have shown the problem of averaging artefacts for double-sided two-way ranging in weak NLOS environments and proposed a method to mitigate this effect. The proposed method enables separate labeling of each packet sent in the double-sided two-way ranging message exchange. The labeling method is applied to the training data and utilizes time information and channel impulse responses to accurately estimate the time-of-flight of individual packets. It was shown that the proposed labeling increases the separation between LOS and NLOS classes in the feature space. In one of the two presented test cases, a detector trained with the proposed labeled data showed significantly better detection results.

References

[1] D. Neirynck, E. Luk, and M. McLaughlin, "An alternative double-sided two-way ranging method," in *13th Workshop Pos., Navig. Commun. (WPNC)*. IEEE, 2016, pp. 1–4.

[2] J. Schroeder, S. Galler, K. Kyamakya, and K. Jobmann, "NLOS detection algorithms for ultra-wideband localization," in *2007 4th Workshop on Positioning, Navigation and Communication*. IEEE, 2007, pp. 159–166.

[3] N. Decarli, D. Dardari, S. Gezici, and A. A. D'Amico, "LOS/NLOS detection for UWB signals: A comparative study using experimental data," in *IEEE 5th International Symposium on Wireless Pervasive Computing 2010*. IEEE, 2010, pp. 169–173.

[4] W. Li, T. Zhang, and Q. Zhang, "Experimental researches on an UWB NLOS identification method based on machine learning," in *15th IEEE Int. Conf. Commun. Technology*. IEEE, 2013, pp. 473–477.

[5] A. Musa, G. D. Nugraha, H. Han, D. Choi, S. Seo, and J. Kim, "A decision tree-based NLOS detection method for the UWB indoor location tracking accuracy improvement," *Int. Journal Commun. Systems*, vol. 32, no. 13, p. e3997, 2019.

[6] M. Stahlke, S. Kram, C. Mutschler, and T. Mahr, "NLOS detection using UWB channel impulse responses and convolutional neural networks," in *2020 Int. Conf. Localization and GNSS (ICL-GNSS)*. IEEE, 2020, pp. 1–6.

[7] S. Marano, W. M. Gifford, H. Wymeersch, and M. Z. Win, "NLOS identification and mitigation for localization based on UWB experimental data," *IEEE Journal on selected areas in communications*, vol. 28, no. 7, pp. 1026–1035, 2010.

[8] A. F. Molisch, K. Balakrishnan, C.-C. Chong, S. Emami, A. Fort, J. Karedal, J. Kunisch, H. Schantz, U. Schuster, and K. Siwiak, "IEEE 802.15. 4a channel model-final report," *IEEE P802*, vol. 15, no. 04, p. 0662, 2004.

[9] J. Khodjaev, Y. Park, and A. Saeed Malik, "Survey of NLOS identification and error mitigation problems in UWB-based positioning algorithms for dense environments," *annals of telecommunications-annales des télécommunications*, vol. 65, no. 5, pp. 301–311, 2010.

[10] J. Park, S. Nam, H. Choi, Y. Ko, and Y.-B. Ko, "Improving deep learning-based UWB LOS/NLOS identification with transfer learning: An empirical approach," *Electronics*, vol. 9, no. 10, 2020.

[11] *DW1000 Data Sheet*, DecaWave Ltd., 2014, version 2.04.

[12] *DW1000 metrics for estimation of non line of sight operating conditions*, DecaWave Ltd., 2016, aPS006 Part 3 Application Note, version 1.1.

[13] P. Peterseil, D. Märzinger, and B. Etzlinger. (2022, Jun.) UWB weak-NLOS structured dataset. [Online]. Available: https://github.com/ppeterseil/UWB-weak-NLOS-structured-dataset

[14] P. J. Bickel and E. Levina, "Some theory for Fisher's linear discriminant function,naive bayes', and some alternatives when there are many more variables than observations," *Bernoulli*, vol. 10, no. 6, pp. 989–1010, 2004.